PHOTOPHYSICAL PROPERTIES OF ANTIMONY-DOPED TIN OXIDE NANOCRYSTALS

[2]Ibiyemi Abideen A., [1]Yusuf Gbadebo T., [2]Faremi Abass A and [1]Lateef K.

[1]Department of Science Laboratory Technology, Osun State Polytechnic, P.M.B 301, Iree, Nigeria,

[2]Department of Physics, Federal University, Oye-Ekiti, Nigeria

ARTICLE INFO

Received: 5 April 2017
Accepted: 20 July 2017

Keywords:
Annealing, doping, spray pyrolysis, tin oxide, resistivity

Corresponding author:
:abideen.ibiyemi@fuoye.edu.ng

Abstract

Transparent conducting antimony-doped tin oxide (Sb:SnO_2) films have been deposited on glass substrates by spray pyrolysis equipment. The optical and electrical properties of the Sb:SnO_2 films have been investigated as a function of Sb-doping level. The optimum target composition for high conductivity and low resistivity was found to be 20 % of Sb in Sb: SnO_2. The electrical resistivity and sheet resistance were found to be 6.2×10^{-4} Ω-cm, and 17.5 Ω/sq, respectively. The average optical transmittance in the visible range and average optical band-gap are of 89 % and 3.96 eV respectively. The films deposited at lower and higher doping concentrations (0% and 30%) show relatively rough, loosely bound and slightly porous surface morphology while the film deposited at moderate doping concentration 20% shows uniformly distributed grains of greater size. The films deposited in this work have good applications in solar cell devices.

1.0 Introduction

Doped tin oxide thin films are widely used as a transparent electrode in optoelectronics devices including liquid crystal displays, solar cells and plasma display panels due to their high electrical conductivity and high optical transmittance in the visible, and high infrared reflectance [1-3]. SnO_2 films are inexpensive, chemically stable in acidic and basic solutions, thermally stable in oxidizing environments at high temperatures, and also mechanically strong, which are important attributes for the fabrication and operation of solar cells. These attributes of course makes SnO_2 films be a preferred as an alternative to the more widely used indium tin oxide (ITO). Many dopants, such as antimony (Sb), arsenic (As), phosphorus (P), indium (In), molybdenum (Mo), fluorine (F), and chlorine (Cl), have been studied to improve the electrical and optical properties of SnO_2 films [1–7]. Among these, S band F was found to be the most commonly used dopant for photovoltaic devicesfrom the manufacturing point of view. A lot of researches have been carried out with Fluorine as dopant. There are, however relatively scanty researches reports about Sb as a source of dopant especially on optimization of annealing temperature and dopant concentration. Highly conductive SnO_2

films can be achieved by substitution of either Sb^{5+} ions at Sn^{4+}cation sites or Sb^{-}ions at O^{2-}anion sites in the lattice, creating extra electron carriers. Sb-doping is preferred because, at moderate doping levels, it tends to form segregated clusters in the lattice, causing a darkening of the films. For this reason, higher mobility values can normally be observed for Sb- doped SnO_2 films resulting in much lower resistivity SnO_2 films without compromising their optical transmittance [7].

Antimony doped tin oxide (Sb:SnO2) thin films are deposited by various methods namely: Chemical Spray [9], RF Magnetron Sputtering [8], Electrolyses Deposition [10], ChemicalMist Deposition (CMD) [11], Spray Pyrolysis [9-11], and Thermal Evaporation[12-14]. However, in order to obtain low resistivity films, these techniques require optimizing some deposition parameters such as doping level, flow rates, and annealing temperature. These treatments limit their use as a top contact layer in amorphous Si-based solar cells and other types of thin-film solar cells. Spray pyrolysis is one of far most economical and reliable methods ofdepositing thin films onto substrates. Thangarajuhave carried out structural and electrical studies on highly conducting spray deposited fluorine and antimony doped SnO**2** thin films from a SnCl2 precursor and reported the lowest sheet resistance (Rsh= 5.65Ω/sq) with 70% transmittance [15]. In 1990, Reddy et al reported that doping of SnO_2 withAntimony improves the electrical and optical properties butreduces the grain size of the polycrystalline films, whichcould lead to an increase of transmission [16]. In this research work, we report on the study of the structural, electrical and optical properties of Sb: SnO_2 thin films deposited by spray pyrolysis technique on glass substrates as a function of Sb-doping level.

2.0 Materials and Methods

9.334 g of $SnCl_4.5H_2O$ analytical grade was dissolved in 10 ml of concentrated hydrochloric acid by heating at 110 ^oC for 15 minutes. The addition of HCl rendered the solution transparent. The transparent solution thus obtained and subsequently diluted by ethanol, which served as the precursor. For Sb doping, antimony trichloride ($SbCl_3$) was dissolved in isopropyl alcohol and then added to the precursor solution. The amount of antimony trichloride ($SbCl_3$) added was varied from 0-30% in step of 10 %. The total amount of spray solution used for each batch was 50 ml. For each concentration, the reproducibility of the films was verified by repeating the experiments several times. Before deposition, the 5.0 cm × 5.0 cm glass substrates were cleaned thoroughly with industrial detergent, rinsed with deionized water followed by acetone, then rinsed again with deionized water, and finally hot-air dried. The film deposition was done by scanning the surface of the vacuum-chucked substrate with the sprayer in cycles. The distance between the spray nozzle and the substrate as well as the spray time was maintained at 5.0 cm and 15 minutes respectively. The thickness of the films was observed to be at the range of $3 - 10\ \mu m$.

In this work, Sb doped tin oxide thin films were deposited by spray pyrolysis method. Process parameters have significant influence in the quality of spray pyrolyzed thin films. These include doping concentration, flow rate, substrate temperature and nozzle-substrate distance. In 1967, Cullity reported that deviation from stoichiometry due to oxygen vacancies makes tin oxide thin films to possess

semiconducting nature [17]. It is very essential that the complete oxidation of the metal should be avoided in order to obtain films with good conductivity. The substrate temperature also plays an important role in the formation of a quality film. When the substrate temperature was below 350 ^{o}C, the spray falling on the substrate underwent incomplete thermal decomposition (oxidation) giving rise to a foggy film whose transparency as well as electrical conductivity will be very poor. Also, when the substrate temperature was too high (> 500 ^{o}C) the spray gets vaporized before reaching the substrate and the film becomes almost powdery. Therefore, in line withpreviousreport, at substrate temperature in the range of 350-500 ^{o}C, the spray reaches the substrate surface in the semi vapour state andallowing for complete oxidation will take place to give clear SnO_2 film as a final product. Keeping these facts in mind, we optimize substrate temperature at 400^{o}C.

A reservoir of reagent solution is maintained at a temperature sufficiently low to inhibit homogeneous reactions. The solution was nebulized into droplets by an ICP/MS nozzle, which was specified by the manufacturer to produce droplets in the size range 5 - 15 μm, and these droplets were sprayed onto the heated substrate. A proportional integral derivative (PID) controlled heater maintained the substrate temperature at 400 °C. A Panalytical Empyrean X-ray diffraction (XRD) system in asymmetric out-of-plane geometry (with 30 kV, 40 mA, Cu K_α radiation at λ = 0.1540598 nm) was used to record the XRD pattern of the fabricated films for 2θ values from 20 to 80 degrees. Scanning electron microscopy (SEM) images were obtained using a Zeiss Ultra 55 SEM at 5 kV to characterize the particle morphologies. A Perkin-Elmer Lambda 900 spectrophotometer collected transmittance spectra *T* over the wavelength range 200 – 1000 nm. Film thickness *d* was determined from cross-sectional SEM. The optical energy bandgap of the material was deduced from the absorption coefficient spectrum. Resistivity, mobility, and carrier concentration were evaluated by Hall Effect measurements at room temperature in a Van der Pauwfour-point probe configuration, using indium contacts, in a Hall Effect system (MMR technologies) with a magnetic induction of 0.65 T.

3.0 Results and Discussion

Fig. 1 shows the X-ray diffraction (XRD) patterns as a function of tin antimony content in the target for undoped SnO_2 (0%) and Sb-doped SnO_2 (0–30%) films. From the figure below, all the films are polycrystalline and contain the SnO_2 tetragonal structure [18]. All the films exhibit the preferred orientation with a (200) planewith the highest intensity reflection corresponding to the (110) peak. Similar (200) preferred orientation has been observed by other groups [11, 12] with Sb:SnO_2 films spray pyrolysis. The grain size of the deposited films was calculated by the Scherer formula [19] from the XRD peaks to be between 23-29 nm. The lattice parameters (a and c) from the XRD patterns for undoped SnO_2 and doped Sb:SnO_2 films were estimated. For all films, the 'a' lattice parameter values are larger than that of the SnO_2 powder (a =4.744 Å), while for the doped films (5–20 %) the 'c' values are larger than that of the SnO_2 powder (c =3.065 Å). The volume of the unit cell is not significantly affected by Sb- doping, but it appears to be larger than that of the SnO_2. Since the ionic radius of Sb^{-} is slightly larger than that of O^{2-}, the small change in the lattice volume is probably due to the incorporation of Sb ions into

the O ion sites. This change of lattice parameters is also related to oxygen deficiency [17] and strain effects due to the thermal expansion coefficient mismatch between the film (5×10^{-6}/ °C) [20]. This observation is also in line with Kim et al [13].

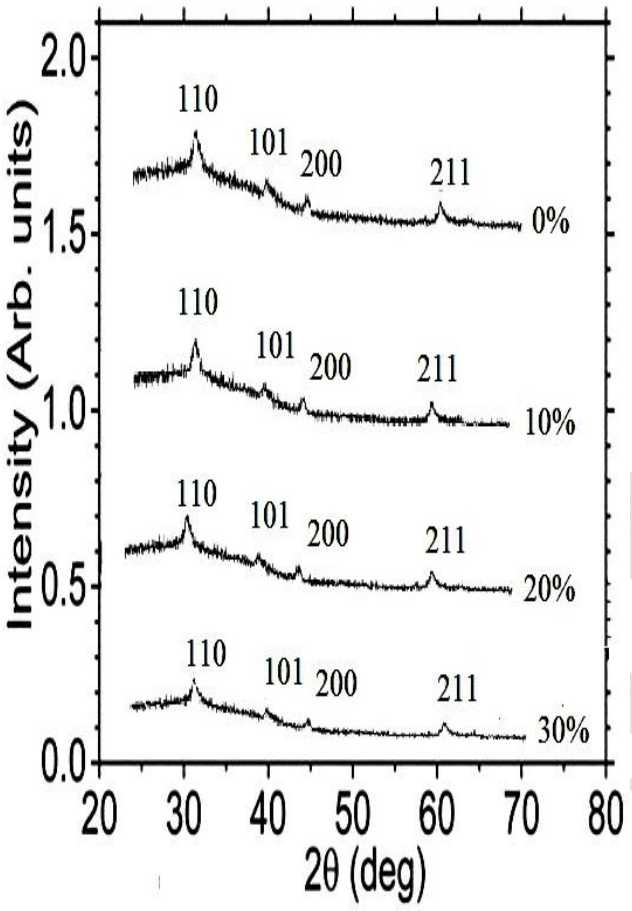

Fig. 1: XRD Analysis of doped Sb:SnO_2

Table 1 shows the electrical properties of the deposited films with differentdoping concentrations.The lowest electrical resistivity of 6.2×10^{-4} Ω-cm and sheet resistance of 17.5 Ω/sq were recorded for sample deposited at 20% of Sb concentration. The resistivity shows an initial decrease reaching a minimum at 20 % doping concentration, and slightly increases as the doping concentration increases.

Table 1: Deposition conditions

Deposition Conditions	Sheet Resistance (Ω/sq)	Resistivity (Ω.cm)	Hall Mobility (cm^2/V.s)
0%	20.1	10.2×10^{-4}	8.92
10%	19.4	9.2×10^{-4}	-8.83
20%	17.5	6.2×10^{-4}	-9.21
30%	18.8	8.1×10^{-4}	-9.02

The initial decrease in resistivity is attributed to an increase in free carrier concentration due to the substitutional incorporation of Sb^{-} ions at O^{2-} anion sites. However, for films with higher doping (30%), the free carrier concentration saturates and the mobility decreases due to the formation of Sn–Sb complexes in the grain boundaries, leading to a slight increase in the resistivity of the SnO_2: Sb films. Figures 2(a)–(d) show the SEM images of Sb:SnO_2 thin films deposited with doped Sb concentration of 0 to 30% in step of 10%. The films deposited at lowest and highest doping concentrations (0 and 30%**)** appear to be have relatively rough texture, loosely bound and slightly porous surface morphology, while the film deposited at moderate10% and 20% doping concentrations shows a fairly uniformly grains distributed with relatively greater sizes. The film is rough, homogenous, compact and adherent in nature**.** The presence of big and faceting nanocrystals observed in Fig. 2b and Fig. 2c for 10% and 20% Sb doping indicates the fact that pyramidal crystallites are formed by coalescence. At lower doping concentrations, randomly oriented spherical grains are observed. At higher (30%) doping levels, these spherical grains are converted into needle-like, prismatic, and

pyramidal- like grains. The observations in this study show a clear morphological dependence on the concentration of the dopant**.** This means that the external shape of the macrocrystals is a combination of prisms (lateral facets of the crystal) and pyramids (end facets of the crystal). The optical transmittance (T) data were used to calculate the absorption coefficient (α) of the films using the relation: $T \approx \exp(-\alpha t)$, where t is the film thickness. The absorption coefficient data was used to determine the optical band-gap (E_g) using the relation: $\alpha h\nu \approx (h\nu - E_g)^{1/2}$, where hν is the photon energy. The direct optical band-gap was determined by extrapolating the straight regions of the plots of α^2 vs. hν to $\alpha^2 = 0$ (i.e., αhν=0) [22]. The transmittance values were observed to slightly decrease with increasing Sb concentration in the films. Fig. 3 shows the variation of transmittance in the UV-visible range (400– 800 nm) as a function of Sb level in SnO_2 films. The transmittance values are observed to slightly increases with increasing Sb concentration in SnO_2 until 20%. **A**30% doping concentration **gave rise to**a decrease in transmittance **typically in 30% doping concentration**was observed. This is probably attributed to an increase of the carrier concentration in the films as a result of Sb doping. Sb: SnO_3 film exhibits average transmittance of 89% in the visible range, and there is a sharp short-wavelength cut-off due to fundamental absorption [13]. These observations are in good agreement with the earlier report [18]. Figure 4 shows the $(\alpha h\nu)^2$ versus photon energy (hν) plot for Sb: SnO_2 films.

Fig. 2: Scanning electron micrographs of Sb: SnO_2 thin films deposited at (a) 0 % (b) 10 % (c) 20% (d) 30% Sb doping concentrations.

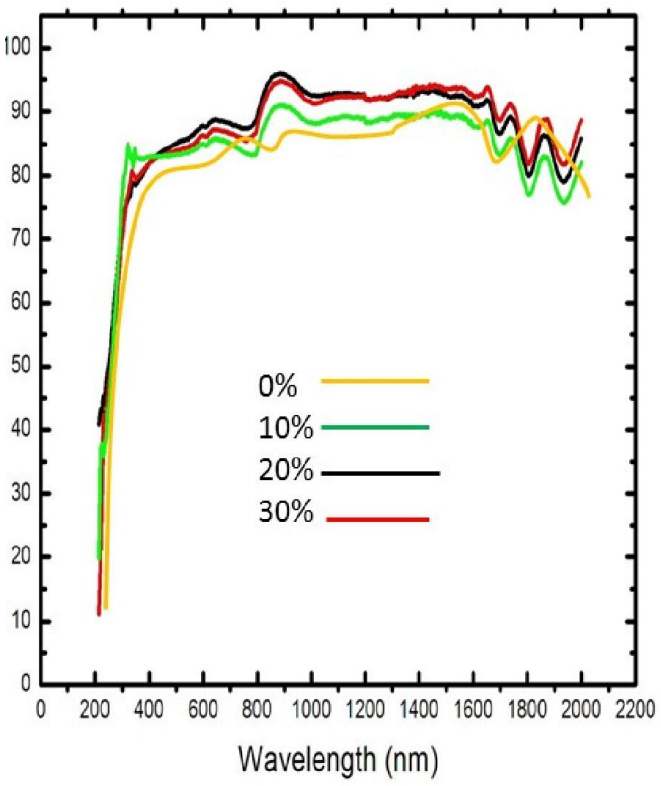

Fig.3: Transmittance curve of percentage Sb doping concentrations in Sb:SnO_2.

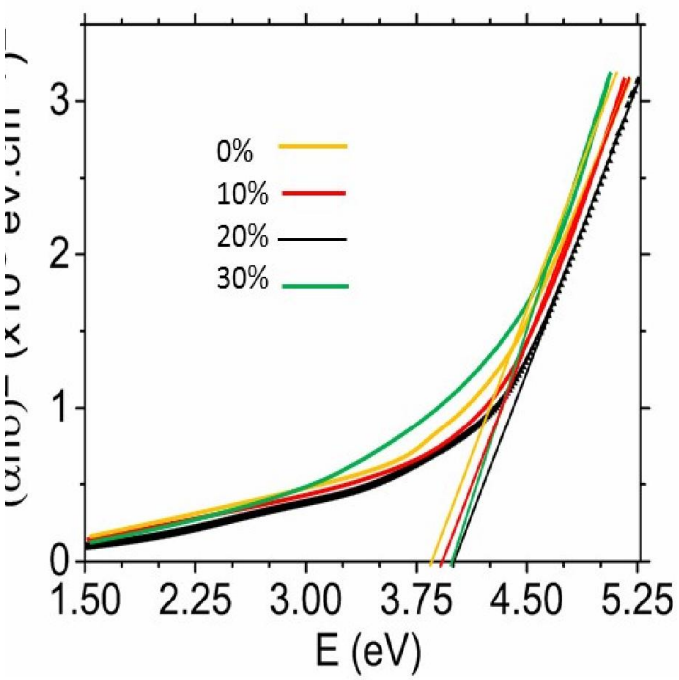

Fig 4: Plot of $(\alpha h\nu)^2$ as a function of photon energy (hν).

The bandgap (E_g) values for the Sb-SnO_2 films (Sb) concentrations 0%, 10%, 20% and 30% are 3.91, 3.93, 4.02 and 4.01 eV respectively obtained from Fig.4. The average optical band-gap (Eg), is 3.96eV. From the figure, it is observed that the bandgap of the films increases with the increase in concentration of antimony Sb with maximum in 20% doping concentration and decreases thereafter.

4.0. Conclusion

High quality Sb:SnO_2 films were grown on glass substrates using spray pyrolysis technique. The electrical and optical properties of the Sb:SnO_2 films were investigated as a function of Sb doping concentration. When the doping concentration increases, the intensity of the (211) peak increases. The Minimum resistivity was observed in Sb: SnO_2 film with 20% doping level, and the transmittance values are observed to slightly decrease with increasing Sb concentration in SnO_2. Further increase in Sb levelto leads increase in resistivity of the film. The resistivity decreases from 0 % doping level to 20%, further increase inSb doping levels however leads to increase in resistivity of the target. An average optical transmittance of 89% in the visible range and average optical band gap of 3.96 eV were measured. The films deposited at lower doping concentration shows a relatively rough, loosely bound slightly porous surface morphology while the film deposited at moderatedoping concentration of 20% shows uniformly distributed grains of greater size. This work has shown the ability to grow Sb:SnO_2 films with low resistivity, high optical transmission and moderate doping concentration. From the above explanations in this work, it is obvious that the best deposited film is that of 20% doping concentration. This is of great importance for the fabrication of high quality transparent electrodes for solar cell applications.

References

[1] Kim H. and Piqué A (2004), Appl. Phys. Lett. 84, pp 218.

[2] Vishwakarma S.R. Upadhyay, Prasad J.P. (1989), Thin Solid Films 176, pp 99.

[3] Upadhyay J.P., Vishwakarma S.R.and Prasad H.C (1988), Thin Solid Films 167, pp 7.

[4] Stjerna V. Olsson and Granqvist , C.G., J. (1994) Appl. Phys. 76 pp 3797.

[5] Manoj, B. Joseph, V.K. Vaidyan, D.S.D (2007) Amma, Ceramic International, pp 273.

[6] Suporthina S., De Guire M.R., Thin Solid Films 371 (2000).

[7] Hartnagel H.L., Dawar A.L., Jain A.K., Jagadish C (1995), Semiconducting Transparent Thin Films, Institute of Physics Publishing, Bristol., pp1-20.

[8] Suzuki K. and Mizuhashi M (1982)., Thin Solid Films.97, pp 119.

[9] Kaneko H. and Miyake K., J (1982), Appl. Phys., 53, pp 3629.

[10]D. Raviendra and J.K. Sharma, J(1985), Phys. Chem. Solids.,46, pp 945.

[11 Lida]H., Mishuku T., Ito A., Kato K., Yamanaka M. and Hayashi Y. (1988), Solar energy Materials, 17, pp 407.

[12] Shanthi E., Dutta V., Banerjee A.and Chopra K. L. (1980), J. Appl. Phys., 51: pp 6243.

[13] Shanthi E., Banerjee A., Dutta V.and Chopra K. L (1982), J. Appl. Phys., 53, pp 1615.

[14]J. Manifacier C., De Murcia M. and Fillard J. P (1977), Thin Solid Films, pp 41, pp 127.

[15] Das D., Banerjee R. (1987), Thin Solid Films, pp 147, 321.

[16] Kim H., Auyeung R.C.Y (2004), A. Piqué, A. Piqué, Appl. Phys. Lett. 84, pp 218.

[17] A.R. Babar, S. S. Shinde, A. V. Moholkar,. Bhosale C. H, and Rajpure K. Y (2011)

[18] Thangaraju B. Structural and electrical studies on highly conducting spray deposited fluorine and antimony doped SnO_2 thin films from $SnCl_2$ precursor. Thin Solid Films, 2002, 402, pp 71

[19] Reddy M. H. M., Jawalekar S. R.and A. N. Chandorkar (1990), Thin Solid Films., 187, pp 171.

[20] Cullity B. D (1967), Elements of x-ray diffraction, second edition, Addison-Wesley publishing company Inc..

[21] Amusan J.A., Olayinka A.S., Nwambo Y.P., Alayande V, Ojuh O.D., James C.C., A. Ibiyemi, Adetunji O.R., Fagbulu A.A and W.B. Ayinde. (2010). Electrical Characterization of Vacuum Thermally Deposited Aluminium Thin Film. Research Journal of Applied Sciences 5, pp 2.

[22]Joint Committee on Powder Diffraction Standards, International Centre forDiffraction Data, # 41-1445.

[23] Cullity B.D. (1978) Elements of X-ray Diffraction, 2nd ed. Addison-Wesley, Reading, MA,.

[24] H. Kaneko, K. Miyake, J. Appl. Phys. 53 (1982) pp 3629.

[25] Tauc J., Grigorovici R., Vancu A., Phys. Status Solid 15 (1966), pp 627.